BENNETT, M. J. & FOXMAN, B. M. (1967). *MMMR, Rigid-body analysis programme*. Massachusetts Institute of Technology, Cambridge, Massachusetts.
BERNDT, A. F. & MARSH, R. E. (1963). *Acta Cryst.* **16**, 118–123.
BIJVOET, J. M. & KETELAAR, J. A. A. (1932). *J. Amer. Chem. Soc.* **54**, 625–628.
BROWN, G. M. & CHIDAMBARAM, R. (1973). *Acta Cryst.* B**29**, 2393–2403.
CHIDAMBARAM, R. & BROWN, G. M. (1973). *Acta Cryst.* B**29**, 2388–2392.
CHURCHILL, M. R. & O'BRIEN, T. A. (1969). *J. Chem. Soc. A*, pp. 1110–1115.
COX, E. G., CRUICKSHANK, D. W. J. & SMITH, J. A. S. (1958). *Proc. Roy. Soc.* A**247**, 1–21.
CRUICKSHANK, D. W. J. (1956). *Acta Cryst.* **9**, 754–756.
CRUICKSHANK, D. W. J. (1960). *Acta Cryst.* **13**, 774–777.
CRUICKSHANK, D. W. J. (1965). *Computing Methods in Crystallography*. Edited by J. S. ROLLETT, pp. 112–116. New York: Pergamon Press.
CRUICKSHANK, D. W. J., JONES, D. W. & WALKER, G. (1964). *J. Chem. Soc.* pp. 1303–1314.
DUCKWORTH, J. A. K., WILLIS, B. T. M. & PAWLEY, G. S. (1970). *Acta Cryst.* A**26**, 263–271.
FOXMAN, B. M. & BENNETT, M. J. (1967). *SFLS5R*, Full-matrix structure-factor and least-squares programme. Massachusetts Institute of Technology, Cambridge, Massachusetts.
HAMILTON, W. C. (1965). *Acta Cryst.* **18**, 502–510.
HAMILTON, W. C., EDMONDS, J. W., TIPPE, A. & RUSH, J. J. (1969). *Discuss. Faraday Soc.* **48**, 192–204.
HARDGROVE, G. L. & TEMPLETON, D. H. (1959). *Acta Cryst.* **12**, 28–32.
HOLM, C. H. & IBERS, J. A. (1959). *J. Chem. Phys.* **30**, 885–888.
HUTCHEON, W. L. (1971). Ph.D. Thesis, Univ. of Alberta.
JOHNSON, C. K. (1969). *Acta Cryst.* A**25**, 187–194.
JOHNSON, C. K. & LEVY, H. A. (1974). In *International Tables for X-ray Crystallography*, Vol. IV. Birmingham: Kynoch Press.
JONES, T. A. (1968). *J. Sediment. Petrol.* **38**, 61–67.
KAY, M. I. & CROMER, D. T. (1970). *Acta Cryst.* B**26**, 1349–1355.
KING, M. V. & LIPSCOMB, W. N. (1950). *Acta Cryst.* **3**, 155–158.
LA PLACA, S. J. & IBERS, J. A. (1965). *Acta Cryst.* **18**, 511–519.
MASLEN, E. N. (1970). In *Crystallographic Computing*, Edited by F. R. AHMED, pp. 231–239. Copenhagen: Munksgaard.
MISES, R. VON (1918). *Phys. Z.* **19**, 490–499.
PAWLEY, G. S. (1963). *Acta Cryst.* **16**, 1204–1208.
PAWLEY, G. S. (1966). *Acta Cryst.* **20**, 631–638.
PAWLEY, G. S. & WILLIS, B. T. M. (1970). *Acta Cryst.* A**26**, 260–262.
PREWITT, C. T. (1966). *SFLS5*, Full-matrix structure factor and least-squares programme. E. I. du Pont de Nemours and Company, Wilmington, Delaware.
SCHOMAKER, V. & TRUEBLOOD, K. N. (1968). *Acta Cryst.* B**24**, 63–76.
SCHUNN, R. A., FRITCHIE, C. J. & PREWITT, C. T. (1966). *Inorg. Chem.* **5**, 892–899.
STEPHENS, M. A. (1963). *Biometrika*, **50**, 385–390.
STEWART, R. F., DAVIDSON, E. R. & SIMPSON, W. I. (1965). *J. Chem. Phys.* **42**, 3175–3187.
WILLIS, B. T. M. & PAWLEY, G. S. (1970). *Acta Cryst.* A**26**, 254–259.

Acta Cryst. (1975). A**31**, 494

Accurate Positional and Thermal Parameters of Hexamethylenetetramine from *K*-Shell X-ray Diffraction Data

BY E. D. STEVENS* AND H. HOPE

Department of Chemistry, University of California, Davis, California 95616, *U.S.A.*

(*Received* 9 *December* 1974; *accepted* 5 *February* 1975)

Geometric and thermal parameters for hexamethylenetetramine have been determined from 95 unique reflections (Mo $K\alpha$, graphite monochromator) in the sin θ/λ range 0·65–1·10 Å^{-1}. Both standard (second cumulant) anisotropic thermal parameters and third cumulant parameters as well as positional parameters for C and N are in excellent agreement with the corresponding neutron parameters. H atom parameters were not determined from the X-ray data. The estimated standard deviations for the X-ray parameters are generally one fifth (or less) of those for the neutron parameters. This study shows that with X-ray data it is possible to determine geometric and thermal parameters free of effects from valence electron asphericity.

Introduction

Recent interest in the experimental determination of molecular electron density distributions has renewed interest in the comparison of X-ray and neutron diffraction results. The aspherical electron distribution of atoms in molecules will influence parameters refined from conventional X-ray data. In a survey, Hamilton (1969) found significant differences between X-ray and neutron results in all cases.

When the positional and thermal parameters deter-

---

* Present address: Department of Chemistry, State University of New York, Buffalo, N.Y. 14214, U.S.A.

mined from neutron diffraction are used with X-ray data to calculate a difference electron density map, the difference density represents the redistribution which occurs as a result of bonding.

An alternative approach in determining electron density distributions is to use parameters refined from high-order X-ray data rather than neutron parameters (Stewart, 1968). An inspection of atomic scattering factors suggests that C and N valence electrons will not contribute significantly to X-ray scattering above 0·65 Å^{-1} (sin θ/λ). If the core electrons are not significantly affected by bonding and if bonding features do not contribute to high-order scattering, the results of an accurate high-order refinement should be free of bias from the aspherical distribution of valence electrons and should show no systematic differences from neutron diffraction results.

X-ray data have been collected from a single crystal of hexamethylenetetramine (HMT) to test the hypothesis that high-order refinements of X-ray data will yield the same results as neutron diffraction data. The accurate neutron diffraction study by Duckworth, Willis & Pawley (1970) is available for comparison.

Experimental

Crystals of hexamethylenetetramine (J. T. Baker Chemical Co.) were grown from a 95% ethanol solution in a convection tube (Hope, 1971*b*). A crystal was ground into a sphere of diameter 0·45 mm, coated with a thin layer of glue to prevent sublimation, and mounted on a Picker automated four-circle diffractometer equipped with an incident-beam graphite monochromator. The angular coordinates ($\chi,\omega,2\theta$) of 15 Mo $K\alpha_1$ reflections were used in a least-squares calculation to determine the crystal orientation and cell dimensions. The cell edge was found to be $a_0=7{\cdot}028\ (2)$ Å at 24°C with $\lambda=0{\cdot}70926$ Å for Mo $K\alpha_1$ radiation.

The positional and thermal parameters determined by neutron diffraction (Duckworth *et al.*, 1970) were used together with sample scan and background measurements to predict which reflections would have measurable X-ray intensities. The setting angles χ, φ, and ω were chosen to minimize the contributions of multiple Bragg scattering using a procedure similar to that of Coppens (1968). For each reflection, a rotation ψ about the diffraction vector was chosen which would avoid contact of all other observed reflections with the sphere of reflection.

The intensities of 1251 selected reflections were measured using a $\theta:2\theta$ scan, graphite monochromatized Mo $K\alpha_1$ radiation, and a scintillation detector with a pulse-height analyzer. Each reflection was scanned from $[2\theta(\alpha_1)-0{\cdot}8°]$ to $[2\theta(\alpha_2)+0{\cdot}7°]$ with a scan speed of $0{\cdot}25°(2\theta)$/min. Background counts were taken for 100 s at each end of the scan range. Coincidence losses were minimized by adding an attenuator filter when the count rate exceeded 10000 c.p.s.

Two check reflections were measured after every 50 reflections and showed a gradual decline in intensity, probably caused by sublimation, amounting to 10% at the end of data collection. A correction for this was obtained from a single linear least-squares fit of the normalized intensities of both check reflections. Each recorded number of counts, N, was assigned a standard deviation $\sigma(N)=[N+(0{\cdot}0065N)^2]^{1/2}$; the factor 0·0065 reproduces the observed variance in the check reflections after correction for decay. Based on the values of $\sigma(N)$ for scan and background counts, e.s.d.'s for the net intensities were calculated.

Lorentz and polarization corrections were applied to the net intensities. The polarization factor includes the polarization by the monochromator crystal (Hope, 1971*a*). Each measured intensity $I_{\rm obs}$ was corrected for first (α_1) and second order (α_2) thermal diffuse scattering included in the scan

$$I_{\rm Bragg}=I_{\rm obs}/(1+\alpha_1+\alpha_2)\ .$$

The correction was calculated using a procedure described by Stevens (1974) which includes the $K\alpha_1$, $K\alpha_2$ wavelength distribution, the elastic anisotropy, and the orientation of the crystal defined by the χ, φ, and ω angles. The elastic constants of HMT have been measured by Haussühl (1958). The horizontal and vertical detector slits each subtended an angle of 1°. Each correction was calculated with a precision of 0·1%. The largest value was 0·30 for α_1 and 0·07 for α_2.

At least six symmetry equivalent forms of each independent reflection were measured. The intensities and e.s.d.'s of the symmetry equivalent forms were used to calculate a weighted average intensity, e.s.d. of the mean, as well as external ('observed') standard deviation for each independent reflection. For most reflections, the external e.s.d.'s were less than the average e.s.d.'s from counting statistics. However, for weak and very strong reflections the external e.s.d.'s were larger.

Refinement

The quantity $\sum w(F_{\rm obs}-K|F_{\rm cal}|)^2$ was minimized in a full-matrix least-squares refinement, with $w=1/\sigma^2$ where σ is the e.s.d. for the mean of each observed structure factor. The data were divided into two groups: a low-order group with $0{\cdot}0<\sin\theta/\lambda\le 0{\cdot}65$ Å^{-1}, and a high-order group with $0{\cdot}65<\sin\theta/\lambda<1{\cdot}10$ Å^{-1}. Both groups were refined separately.

Refinements were performed with two descriptions of the thermal motion, (1) with conventional anisotropic thermal parameters where the structure factor is given by

$$F_c^{(2)}=\sum_p f^{(p)}\exp\,(2\pi i x_i^{(p)}h_i)\,\exp\,[-\tfrac{1}{4}(B_{ij}a_i^*a_j^*h_ih_j)],$$

and (2) with third cumulant thermal parameters (Johnson, 1969), where the structure factor is given by

$$F_c^{(3)}=\sum_p F_c^{(2,p)}\exp(-iC_{ijk}^{(p)}a_i^*a_j^*a_k^*h_ih_jh_k)\ \ (i,j,k=1,2,3),$$

where $\sum_p$ implies summation over all atoms in the unit cell, the subscripts *i*, *ij* and *ijk* imply single, double and triple summation, respectively and $F_c^{(2,p)}$ is the single-atom contribution to $F_c^{(2)}$. The other symbols have their conventional meanings.

Refinements of type (1) were carried out with both relativistic Hartree–Fock (RHF) and Slater-type orbital form factors.

Scattering factors calculated by Doyle & Turner (1968) were used for nitrogen and carbon. The contracted spherical scattering factor calculated by Stewart, Davidson & Simpson (1965) was used for hydrogen.

During initial refinement, inspection of the deviations between F_o and F_c indicated secondary extinction in the 011 reflection, which has an intensity more than four times greater than the intensity of the next strongest reflection. The reflection was not included in further refinements. All other reflections were considered to be 'observed'.

Since hydrogen does not scatter sufficiently at high angles hydrogen parameters in the high-order refinement were fixed at the values determined by neutron diffraction. The results of type (1) refinements of the X-ray data are compared with the neutron diffraction results in Table 1. Molecular optimized scattering factors (MOSTO) for carbon and nitrogen were calculated from Slater-type orbital exponents optimized to the methane and ammonia molecules, respectively, by Hehre, Stewart & Pople (1970).

The results of refinement of the X-ray data with third-cumulant thermal parameters are compared with a third-cumulant refinement of the neutron data in Table 2. A significant improvement in the model results from third cumulant refinements for both high- and low-order data, as judged by Hamilton's (1965) *R*-factor ratio test.

The parameters from each of the X-ray refinements are compared with the neutron diffraction results using the chi-squared test of Hamilton (1969). Included in each table is the value of χ^2 required for differences in the parameters to be significant at the 0·05 level.

Table 3 gives a comparison of F_o and F_c. The calculated structure factors are based on the high-order refinement with standard anisotropic temperature factors, using RHF form factors.

Discussion

The differences between the low-order X-ray parameters and the neutron parameters are significant and can be attributed to the aspherical distribution of valence electrons. Surprisingly, in our study the nitrogen is not displaced towards the lone pair, in contrast to the results of the previously reported X-ray work (Becka & Cruickshank, 1963).

The hypothesis that the differences between the high-order X-ray parameters and neutron parameters are due to random errors cannot be rejected as indicated by the χ^2 test. In this structure, the nuclear positions and thermal parameters coincide with those

Table 1. *Comparison of refinements with standard (second-cumulant) temperature factors*

Form factor	RHF	RHF	MOSTO	MOSTO	Neutron
Sin θ/λ range (Å^{-1})	0·0–0·65	0·65–1·10	0·0–0·65	0·65–1·10	0·0–0·8
Number of parameters	14	8	14	8	14
Number of reflections	54	95	54	95	49
R (%)	2·86	6·35	2·49	6·31	2·33
R_w (%)	3·55	3·76	3·23	3·68	
Goodness of fit	12·96	3·31	11·74	3·41	
Scale for F_o	0·0258 (1)	0·0280 (1)	0·0280 (1)	0·0279 (1)	
χ^2_{obs}	187·1	4·4	185·5	5·2	
$\chi^2_{0,05}$	22·4	14·1	22·4	14·1	
$(\varphi_X-\varphi_N)_{\text{r.m.s.}}$*	1·62°	1·88°			
Nitrogen					
x,y,z	0·1223 (1)	0·1223 (1)	0·1221 (1)	0·1223 (1)	0·1222 (2)
$B_{11,22,33}$	4·13 (3)	3·84 (2)	3·74 (2)	3·80 (2)	3·87 (6)
$B_{12,13,23}$	−0·79 (2)	−0·83 (1)	−0·77 (1)	−0·83 (1)	−0·81 (6)
Carbon					
x	0·2382 (1)	0·2378 (1)	0·2384 (1)	0·2378 (1)	0·2370 (5)
B_{11}	2·53 (2)	2·11 (2)	2·34 (2)	2·08 (2)	2·04 (12)
$B_{22,33}$	5·40 (3)	5·04 (3)	5·25 (3)	5·01(3)	5·11 (12)
B_{23}	0·27 (4)	0·04 (3)	−0·35 (4)	0·04 (3)	0·02 (20)
Hydrogen					
x,y	0·0898 (8)	[0·0909]	0·0905 (7)	[0·0909]	0·0909 (6)
z	−0·3187 (7)	[−0·3266]	−0·3215 (7)	[−0·3266]	−0·3266 (7)
$B_{11,22}$	7·36 (36)	[8·77]	6·73 (32)	[8·77]	8·77 (28)
B_{33}	3·42 (21)	[4·07]	3·68 (20)	[4·07]	4·07 (22)
B_{12}	−0·66 (32)	[−0·42]	−1·43(27)	[−0·42]	−0·42 (32)
$B_{13,23}$	4·06 (21)	[1·88]	4·43 (19)	[1·88]	1·88 (16)

* φ_X and φ_N are X-ray and neutron phase angles respectively.

Table 2. *Comparison of refinements with third-cumulant temperature factors*

Form factor	RHF	RHF	Neutron
Sin θ/λ range (Å^{-1})	0·0–0·65	0·65–1·10	0·0–0·8
Number of parameters	25	13	25
Number of reflections	54	95	49
R(%)	1·46	5·21	1·18
R_w(%)	1·26	2·39	
Goodness of fit	4·47	2·28	
Scale for F_o	0·0260 (1)	0·0273 (1)	
χ^2_{obs}	166·4	6·4	
$\chi^2_{0,05}$	36·4	21·0	
Nitrogen			
x,y,z	0·1221 (1)	0·1224 (2)	0·1225 (4)
$B_{11,22,33}$	4·06 (1)	3·88 (2)	3·89 (6)
$B_{12,13,23}$	−0·81 (1)	−0·83 (1)	−0·81 (6)
$C_{111,222,333}$	0·027 (6)	0·031 (4)	0·028 (55)
$C_{112,113,122}$ $_{133,223,233}$	−0·013 (2)	−0·012 (2)	−0·003 (35)
C_{123}	0·104 (5)	0·020 (2)	−0·007 (55)
Carbon			
x	−0·2369 (2)	0·2358 (2)	0·2356 (8)
B_{11}	2·40 (2)	2·14 (1)	2·00 (12)
$B_{22,33}$	5·45 (1)	5·13 (2)	5·02 (12)
B_{23}	−0·22 (2)	0·01 (2)	−0·02 (16)
C_{111}	−0·004 (10)	−0·024 (5)	−0·111 (49)
$C_{122,233}$	−0·052 (4)	−0·046 (2)	−0·055 (35)
C_{123}	[0·00]	[0·00]	[0·000]
Hydrogen			
x,y	0·0874 (8)	[0·0904]	0·0904 (8)
z	−0·3155 (8)	[0·3229]	−0·3229 (12)
$B_{11,22}$	8·09 (20)	[8·60]	8·60 (24)
B_{33}	3·15 (17)	[4·60]	4·60 (24)
B_{12}	0·46 (20)	[0·51]	−0·51 (24)
$B_{13,23}$	3·18 (17)	[2·00]	2·00 (14)
$C_{111,222}$	0·083 (97)	[−0·166]	−0·166 (94)
C_{333}	0·086 (83)	[0·253]	0·253 (90)
$C_{112,122}$	0·149 (61)	[0·000]	0·000 (55)
$C_{113,223}$	0·504 (44)	[0·219]	0·219 (69)
$C_{133,233}$	0·203 (35)	[0·142]	0·142 (55)
C_{123}	0·021 (65)	[0·045]	0·045 (62)

of the core electrons determined by the high order X-ray scattering.

The goodness of fit parameter,

$$S=[\sum w(\Delta F)^2/(n-m)]^{1/2}$$

for the high-order refinement is considerably closer to the value of 1·0 expected if model errors are insignificant. This is attributed to the fact that the spherical-atom model used in the refinement is a better representation of the electron distribution in the high-order refinement where the scattering is due to the core electrons.

Table 3. *Observed and calculated structure amplitudes*

F_c is based on second cumulant refinement of high-order data. L denotes low-order data. The columns are l, $100|F_o|$, $100|F_c|$ and $1/\sigma(F_o)$.

```
H= 0, K= 0
 2  1860L  1762   22
 4    28L     6   89
 6    34L    58   32
 8   874L   897   26
10    20     22   40
12    24     26   32

H= 0, K= 1
 3   325L   303  179
 5   103L    95  179
 7   260L   275   71
 9   398L   386   71
11   123    133   89
13    42     49   26
15    27     27   20

H= 0, K= 2
 2  1533L  1446   40
 4   603L   576   51
 6   297L   309  119
 8   221L   246  119
10   145    156   71
12    56     54   30

H= 0, K= 3
 3  1107L  1001   30
 5   939L   944   27
 7   212L   206  179
 9    26     23   32
11    48     51   51
13    80     79   40
15    32     27   18

H= 0, K= 4
 4  2283L  2217   15
 6   186L   185   51
 8    45L    59   60
10    59     53   36
12   114    111   51

H= 0, K= 5
 5   707L   724   46
 7   170L   198   40
 9    34     55   19
13    46     53   26

H= 0, K= 6
 6   320L   308  119
 8    31     42   40
10    30     14   40

H= 0, K= 7
 7    35     21   11
 9   113    115   71
11    33     27   22

H= 0, K= 8
 8   219    212   51

H= 0, K= 9
 9    60     66   26

H= 1, K= 1
 2  2306L  2090   12
 4   108L    74   30
 6   511L   499   51
 8   441L   461   71
10   132    148   45
12    20     33   30
14    31     28   17

H= 1, K= 2
 3  1556L  1468   45
 5   487L   456  119
 7   441L   439  119
 9   109    111   45
11   149    143  179
13    52     56   51
15    28     36   26

H= 1, K= 3
 4  1061L  1036   51
 6   445L   464   89
 8    19L    22   30
10   161    156   89
12    76     76   71

H= 1, K= 4
 5   866L   868   36
 7   146L   167   71
 9    60     68   71
11    28     17   30
13    62     65   45
15    17     25   18

H= 1, K= 5
 6   257L   245   71
 8    66     73   45
10    59     54   40
12    66     63   51

H= 1, K= 6
 7   270    287   89
 9    54     58   89
11    50     50   40
13    23     16   26

H= 1, K= 7
 8   113    101   60
10    50     48   26

H= 1, K= 8
 9   102    101   45

H= 2, K= 2
 2  4226L  4037    3
 4   405L   376  179
 6  1008L  1059   60
 8    68L    51   32
10   239    241   71
12    30     38   32
14    29     32   32

H= 2, K= 3
 3  1275L  1148   60
 5   466L   480   89
 7   413L   434   89
 9   120    125   60
11    95     96  119
13    48     45   27
15    24     28   30

H= 2, K= 4
 4   472L   472   60
 6   260L   270   89
 8   166    161   89
10    50     56   30
12    48     47   24

H= 2, K= 5
 5   186L   175  119
 7   248L   244   89
 9    74     77   36
11    68     68   24
13    22     23   36

H= 2, K= 6
 6   501L   487   71
 8    33     33   40
10   115    113   71

H= 2, K= 7
 7   126    128   89
 9    71     71   27
11    48     51   27

H= 2, K= 8
 8    92     63   89

H= 2, K= 9
 9    17     11   27

H= 3, K= 3
 4   272L   260  119
 6   497L   532  119
 8   235L   240  119
10    80     87   45

H= 3, K= 4
 7   120L   160   45
 9   231    265  119
11    55     59   22
13    25     18   22

H= 3, K= 5
 6   259L   249  119
 8   237    235   89
10    70     68   45

H= 3, K= 6
 7   138    137   40
 9    64     68   60
11    75     72   40

H= 3, K= 7
 8    43     39   40
10    71     78   51

H= 4, K= 4
 4   153L   109  179
 6    63L    80   19
 8   432    429   89

H= 4, K= 5
 5    70L   110   36
 7   189    194   89
 9   145    158   71
11    57     61   40

H= 4, K= 6
 6    45     44   60
 8    61     68   36
10    76     71   32

H= 4, K= 7
 7    65     60   24

H= 5, K= 5
 6    76     69   89
 8   165    182   51
10    66     52   32

H= 5, K= 6
 7   119    117  119
 9    41     19   36
11    42     48   36

H= 5, K= 7
10    53     50   71

H= 6, K= 6
 6   218    218  179
10    69     76   51

H= 6, K= 7
 7   106    122   51

H= 8, K= 8
 8    64     61   30
```

The third-cumulant refinement of low-order X-ray data yields parameters which are significantly different from the parameters of the third cumulant neutron refinement. The third-cumulant parameters are expected to be strongly influenced by the valence electron density distribution. The high-order X-ray parameters, however, are not significantly different from the neutron values. The ability of a refinement of high-order X-ray data to reproduce the positional and thermal parameters determined by neutron diffraction even when third-cumulant thermal parameters are refined indicates that, in this case, bonding features such as lone pairs do not contribute to high-order scattering and the core electrons are not influenced by the valence electron distribution.

The difference between X-ray scale factors refined in the low- and high-order refinements is primarily due to the use of atomic scattering factors calculated from isolated-atom Hartree–Fock wavefunctions. When scattering factors are used which have been calculated from molecular optimized Slater-type orbitals there is no significant difference in the X-ray scale factors.

The low-order X-ray refinement with molecular optimized atomic scattering factors gives better agreement with the neutron refinement than the refinement with Hartree–Fock scattering factors. The agreement of the high-order refinement is not affected.

A difference electron density map calculated from X-ray data and neutron positional and thermal parameters should show the redistribution of electron density in a molecule as a result of bonding. The appearance of the map is strongly dependent on the scale factor used for the X-ray data. The scale factors determined from high-order refinements and from the low-order refinements using molecular optimized atomic scattering factors agree within experimental error with an experimental measurement of the scale factor (Stevens & Coppens, 1974).

A difference density map calculated with the X-ray data and neutron positional and thermal parameters is plotted in Fig. 1(*a*). The unique section of the (110) plane is shown with the carbon–nitrogen bond indicated at the top of the figure and the carbon–hydrogen bond indicated at the bottom. The threefold axis lies in the plane and passes through the upper left corner and lower right corner.

The lone-pair density of the nitrogen atom is clearly visible extending from the nitrogen along the threefold axis. Bonding density is also present in the carbon–nitrogen and carbon–hydrogen bond region.

A difference density map calculated with the X-ray data and the positional and thermal parameters from the high-order X-ray refinement is plotted in Fig. 1(*b*). Since there is no significant difference in the results of the neutron and the high-order X-ray refinements, the difference density maps are nearly identical.

HMT has been used in a joint refinement of X-ray and neutron data in which separate positional parameters and common thermal parameters are refined (Duckworth, Willis & Pawley, 1969). Since the thermal parameters obtained from low-order X-ray data show greater bias due to the valence electrons than the positional parameters, these results indicate that a joint refinement with common positional parameters and separate thermal parameters would be more appropriate, although, in our opinion, the exact interpretation of the results of such refinements would be so difficult as to render them nearly useless. We do not recommend this procedure.

In this case it has been possible, using *K*-shell X-ray diffraction data, to obtain accurate positional and thermal parameters which are not biased by the aspherical distribution of valence electrons. In other cases (*e.g.* structures with oxygen atoms) scattering from lone-pair electrons may extend beyond a sin θ/λ value of 0·65 Å^{-1}, requiring higher-order data.

Support from the National Science Foundation is gratefully acknowledged.

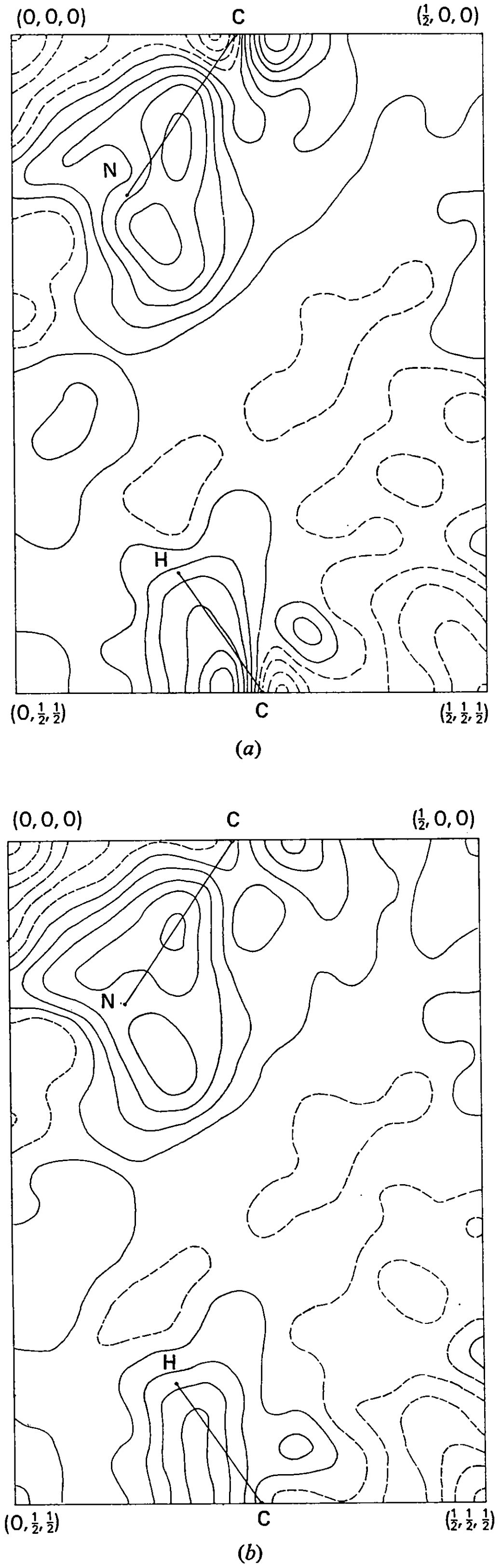

Fig. 1. Difference electron density, 110 plane (*a*) X–N difference map. (*b*) X–X (high-order) difference map.

References

Becka, L. N. & Cruickshank, D. W. J. (1963). *Proc. Roy. Soc.* A**273**, 435–454.

Coppens, P. (1968). *Acta Cryst.* A**24**, 253–257.

Doyle, P. A. & Turner, P. S. (1968). *Acta Cryst.* A**24**, 390–397.

Duckworth, J. A. K., Willis, B. T. M. & Pawley, G. S. (1969). *Acta Cryst.* A**25**, 482–484.

Duckworth, J. A. K., Willis, B. T. M. & Pawley, G. S. (1970). *Acta Cryst.* A**26**, 263–271.

Hamilton, W. C. (1965). *Acta Cryst.* **18**, 502–510.

Hamilton, W. C. (1969). *Acta Cryst.* A**25**, 194–206.

Haussühl, S. (1958). *Acta Cryst.* **11**, 58–59.

Hehre, W. J., Stewart, R. F. & Pople, J. A. (1970). *J. Chem. Phys.* **52**, 2769–2773.

Hope, H. (1971*a*). *Acta Cryst.* A**27**, 392–393.

Hope, H. (1971*b*). *J. Appl. Cryst.* **4**, 333.

Johnson, C. K. (1969). *Acta Cryst.* A**25**, 187–194.

Stevens, E. D. (1974). *Acta Cryst.* A**30**, 184–189.

Stevens, E. D. & Coppens, P. (1974). Unpublished result.

Stewart, R. F. (1968). *J. Chem. Phys.* **48**, 4882–4889.

Stewart, R. F., Davidson, E. R. & Simpson, W. T. (1965). *J. Chem. Phys.* **42**, 3175–3187.